

Influences of Magnetic Flux Density on Discharge Characteristics of Low-Power Hall Thruster

Weilong Guo^{1,*} , Jun Gao¹ , Zuo Gu¹ , Ning Guo¹ 

1. China Academy of Space Technology – Lanzhou Institute of Physics – Science and Technology on Vacuum Technology and Physics Laboratory – Lanzhou/Gansu – China

*Correspondence author: 1347458669@qq.com

ABSTRACT

The design of the magnetic field is crucial to the performance of the hall thruster. This paper investigates the effects of magnetic field on the discharge characteristics of the low-power hall thruster in the method of combining simulation and experiment. Based on a 40-mm-diameter hall thruster (LHT-40) operating with hundreds of Watts, a two-dimensional axisymmetric model is established in fluid method to investigate the mechanism, how the magnetic field influences the performance of the thruster, and the experiments are also carried out to investigate the performance effected by magnetic field. Both the numerical and the experimental results indicate that there is an optimal magnetic flux density in which the thruster could achieve a higher efficiency compared with other conditions. And in order to maintain its high efficiency, the line of magnetic-curve inflexion inside the discharge channel should coincide with the center line of the channel to decrease the interaction between the plasma and the wall. The LHT-40 could generate about 12.2 mN of thrust at an optimal efficiency of 27% when the maximum magnetic flux density along the center line of the channel is about 200 Gs.

Keywords: Magnetic field; Discharge characteristics; Hall thruster.

INTRODUCTION

With the characteristics of the higher specific impulse and the ability to operate in a wide range of power (Conversano *et al.* 2014), hall thrusters are attractive for a wide range of space missions. Especially low-power hall thrusters working under a few hundred Watts have attracted much attention in the field of small satellite (Grimaud *et al.* 2016; Smirnov *et al.* 2002; Zhang *et al.* 2018).

As a propulsion instrument controlled by $E \times B$ field, the ionization and acceleration in the discharge channel of hall thruster is directly influenced by the electromagnetic field on the plasma. To some extent, the performance changes of the hall thruster are the consequence of the variation of the magnetic configuration. Therefore, the design of the magnetic field plays an important role for the performance of the thruster. Some researches have been conducted on the effects of the magnetic field on performance of the hall thruster.

Morozov *et al.* (1972) found that the magnetic flux density along the discharge channel should maintain a negative gradient so that the thruster could operate stably and maintain high efficiency. And then Morozov conducted an experiment to verify his theory based on a stable plasma thruster (SPT) type hall thruster. Hofer and Gallimore (2002) investigated the effect of the magnetic

Received: Jun. 14, 2021 | Accepted: Oct. 20, 2021

Peer Review History: Single Blind Peer Review.

Section editor: José Atilio Fidel Fritz Rocco



This is an open access article distributed under the terms of the Creative Commons license.

configuration under different discharge voltage on the performance of the thruster based on a 20-kW hall thruster named NASA-173M, which was improved via adopting additional coils behind the anode to adjust the magnetic field in the discharge channel. Meanwhile, Hofer (2004) mainly focused on the magnetic configuration but did not pay enough attention to the magnetic flux density. Garrigues *et al.* (2003) studied the effect of the gradient of the magnetic flux density on the plasma characteristics through simulation, and the results infer that the large enough gradient is beneficial to reduce the oscillation of the discharge current.

Hofer and Gallimore (2002) investigated the effect of the magnetic configuration under different discharge voltage on the performance of the thruster based on a 20-kW hall thruster named NASA-173M, which was improved via adopting additional coils behind the anode to adjust the magnetic field in the discharge channel. Meanwhile, Hofer and Gallimore (2012) mainly focused on the magnetic configuration but did not pay enough attention to the magnetic flux density. Garrigues *et al.* (2003) studied the effect of the gradient of the magnetic flux density on the plasma characteristics through simulation, and the results infer that the large enough gradient is beneficial to reduce the oscillation of the discharge current. Gao *et al.* (2016) modified the magnetic configuration near the anode and carried out a series of comparative tests on a cylindrical hall thruster, and found that decreasing the magnetic field near the anode could enhance the propellant utilization. Grimaud and Mazouffre (2018) investigated the effects of the magnetic shielded configuration and the material of the walls on the performance of the hall thruster via experiments.

Owing to inherently larger surface-to-volume ratios compared to the kilowatt class hall thruster (Grimaud *et al.* 2016; Zhang *et al.* 2018), the interaction between the plasma and the discharge channel wall is also larger, consequently, in low-power hall thruster, which will decrease the efficiency. Therefore, the magnetic field of the low-power hall thruster needs to be optimized to ensure its efficiency and the reliability. But research about the effect of the magnetic flux intensity and its radial distribution on the discharge characteristic of the low-power thruster is still inadequate.

This paper focuses on a 40 mm-diameter hall thruster, which is designed to operate from 200 to 300 W, to understand the mechanism of how magnetic field influences the performance, and both the numerical and experimental methods are adopted.

PHYSICAL MODEL AND BOUNDARY CONDITIONS

Computational region

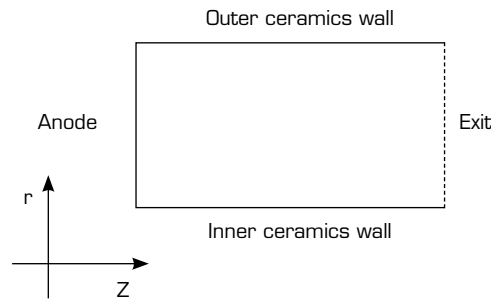
Figure 1 shows the hall thruster focused in this paper, named LHT-40, which has a circular discharge channel. The inner and outer walls of the discharge channel are made of boron nitride ceramics. Magnetic components (coils, shielding and so on), as well as metal anode, build the electromagnetic field in the channel that controls the process of ionization and acceleration.

Taking the centerline of the annular channel as axial, a two-dimensional axisymmetric model is established. Given that the plasma is generated and ejected in the discharge channel, this part is chosen as the simulation region, as shown in Fig. 2. The left side of the channel is the anode, and the right side is the free boundary where ions are ejected. The upper and lower boundaries are ceramic walls.



Source: Elaborated by the authors.

Figure 1. The LHT-40 hall thruster.



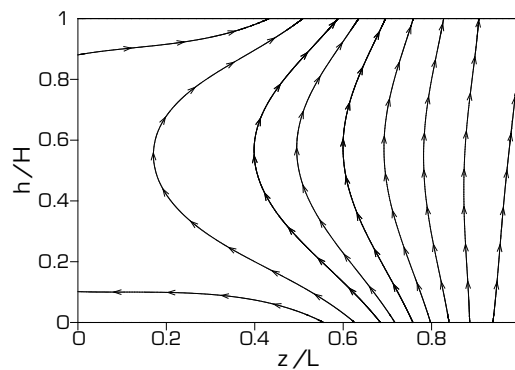
Source: Elaborated by the authors.

Figure 2. Simulation region.

The geometric dimensions of the discharge area have been normalized. In the following text, L represents the length of the discharge channel, z represents the axial position, H represents the width of the discharge channel, and h represents the radial position.

Magnetic field and spatial potential

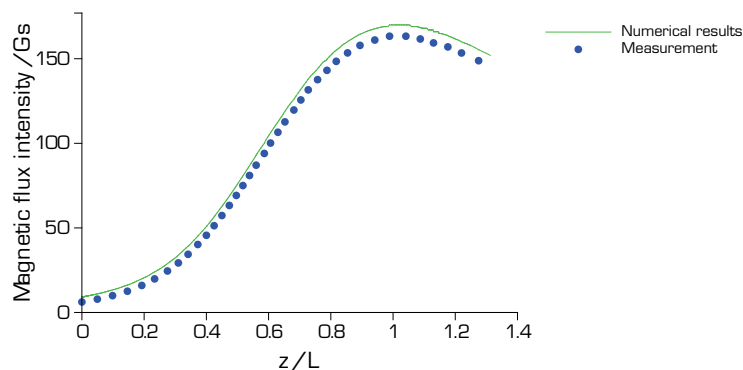
Compared to the magnetic flux density as high as hundreds Gauss generated by coils, that produced by plasma is only a few Gauss, which could be neglected. Figure 3 depicts the magnetic field in the discharge channel of LHT-40 with excitation current of inner and coil at 2.7 and 1.17 A, respectively, which is precomputed by Comsol Multiphysics software.



Source: Elaborated by the authors.

Figure 3. Magnetic configuration in the discharge channel of the hall thruster.

The numerical results and the measurement of the magnetic flux intensity along the discharge channel are shown in Fig. 4, B_r is used to represent that. It can be observed that the B_r is larger near the exit while as low as zero Gs near the anode. The numerical result is almost consistent with the measurement, which means that the numerical result of the magnetic field is reliable.



Source: Elaborated by the authors.

Figure 4. Magnetic flux intensity along the discharge channel of the hall thruster.

The magnetic configuration in this section will be used as a reference magnetic field to investigate the effects of magnetic flux density on the performance of LHT-40 hall thruster in the following text.

The electric field E can be calculated from the derivative of the spatial potential Φ , which is resolved via Poisson's equation shown in Eq. 1, where n_i denotes the ion density while n_e denotes the electron density correspondingly (Duan *et al.* 2016).

$$-\nabla^2\Phi = \frac{e}{\varepsilon_0}(n_i - n_e) \quad (1)$$

PLASMA MOTIONS

In this section, fluid method is used to investigate the discharge characteristic in different magnetic configuration based on the two-dimensional coaxial symmetric model established before. The plasma is generated by collision between electrons and atoms. Therefore, the electrons obey the electron continuity equation (Escobar and Ahedo 2015; Yim *et al.* 2006) and the conservation of electron energy equation (Book 1987; Escobar and Ahedo 2015; Wang *et al.* 2020) given by Eqs. 2 and 3, respectively, where V_e represents the velocity of electrons, k_j and ε_j are included to denote the reaction rate and the energy loss in the reaction. T_e is the so-called electron temperature, describing the average energy of electrons in eV . μ_e is electron mobility rate shown in Eq. 4, where ν denotes the collision frequency between electrons and atoms, and Ω_e denotes the electron hall correction which can be expressed as $\sqrt{\frac{eB}{mV_e}}$ (Book 1987; Katz *et al.* 2004).

$$\frac{\partial}{\partial t}(n_e) - \nabla[V_en_e + \mu_e T_e \cdot \nabla n_e] = \sum_{j=1}^M k_j n_n n_e \quad (2)$$

$$\frac{\partial}{\partial t}\left(\frac{3}{2}n_e T_e\right) + \nabla \cdot \left(-\frac{5}{2}n_e T_e V_e - \frac{5}{2}n_e \mu_e T_e \nabla(T_e)\right) - en_e V_e E - T_e V_e \cdot \nabla n_e = \sum_{j=1}^P k_j n_n n_e \cdot \varepsilon_j \quad (3)$$

$$\mu_e = \frac{e}{m_e \nu (1 + \Omega_e^2)} \quad (4)$$

Reaction rate k_j , shown in Eq. 5, could be obtained by averaging of corresponding cross section (<https://fr.lxcat.net/home/>) with electron energy distribution function, which obey Maxwell distribution, as shown in Eq. 6.

$$k_j = \sqrt{\frac{2e}{m_e}} \cdot \int_0^\infty \varepsilon \sigma_j(\varepsilon) f(\varepsilon) d\varepsilon \quad (5)$$

$$f(\varepsilon) = \frac{2}{\sqrt{\pi} T_e^{3/2}} \exp\left(-\frac{\varepsilon}{T_e}\right) \quad (6)$$

Boundary conditions

The anode of the thruster is the boundary of the conductor and the potential is fixed. The wall of the thruster channel is an insulating wall, usually boron nitride (BN) ceramic material. The electric field perpendicular to the wall can be obtained through the surface charge density. The potential of the anode is set to discharge voltage. The exit of the thruster channel is a vacuum boundary, of which the potential is set to zero volts, and all particles reaching the exit are regarded as ejected.

The electrons arriving at the wall of the discharge channel follow the boundary conditions in Table 1. The walls and anode for ions are the surface reactions boundary conditions (Bird *et al.* 2013; Christou and Jugroot 2014; 2017). Γ_e is the flux of the electrons, n is a unit vector of normal to the boundary, ps is the surface charge, ji and je denote the ion and electron current incident on the boundary, kb is Boltzmann constant and Vd is the anode voltage of the hall thruster.

Table 1. Boundary conditions.

Boundary	n_e
Inner wall	$n \cdot \Gamma_e = \frac{T_e}{35} \sqrt{\frac{8k_b}{\pi m_e}} n_e$
Outer wall	$n \cdot \Gamma_e = \frac{T_e}{35} \sqrt{\frac{8k_b}{\pi m_e}} n_e$
Anode	$n \cdot \Gamma_e = \frac{1}{2} \sqrt{\frac{8k_b T_e}{\pi m_e}} n_e$

Source: Elaborated by the authors.

NUMERICAL SIMULATION RESULTS IN HALL THRUSTER DISCHARGE CHANNEL

Effects of the magnetic flux density on the distribution of electron density and potential

In order to illustrate the effects brought by magnetic flux density, simulation was conducted in different magnetic flux density. Four kinds of magnetic flux density were employed in the simulation, in which the maximum strength along the center line of the discharge channel is 110, 170, 200 and 230 Gs, respectively (Fig. 5). Here, *Br-max* represents these. The initial electron temperature is 2 eV and the density is $1.0 \times 10^{18} \text{ m}^{-3}$. The anode voltage is set to 300 V.

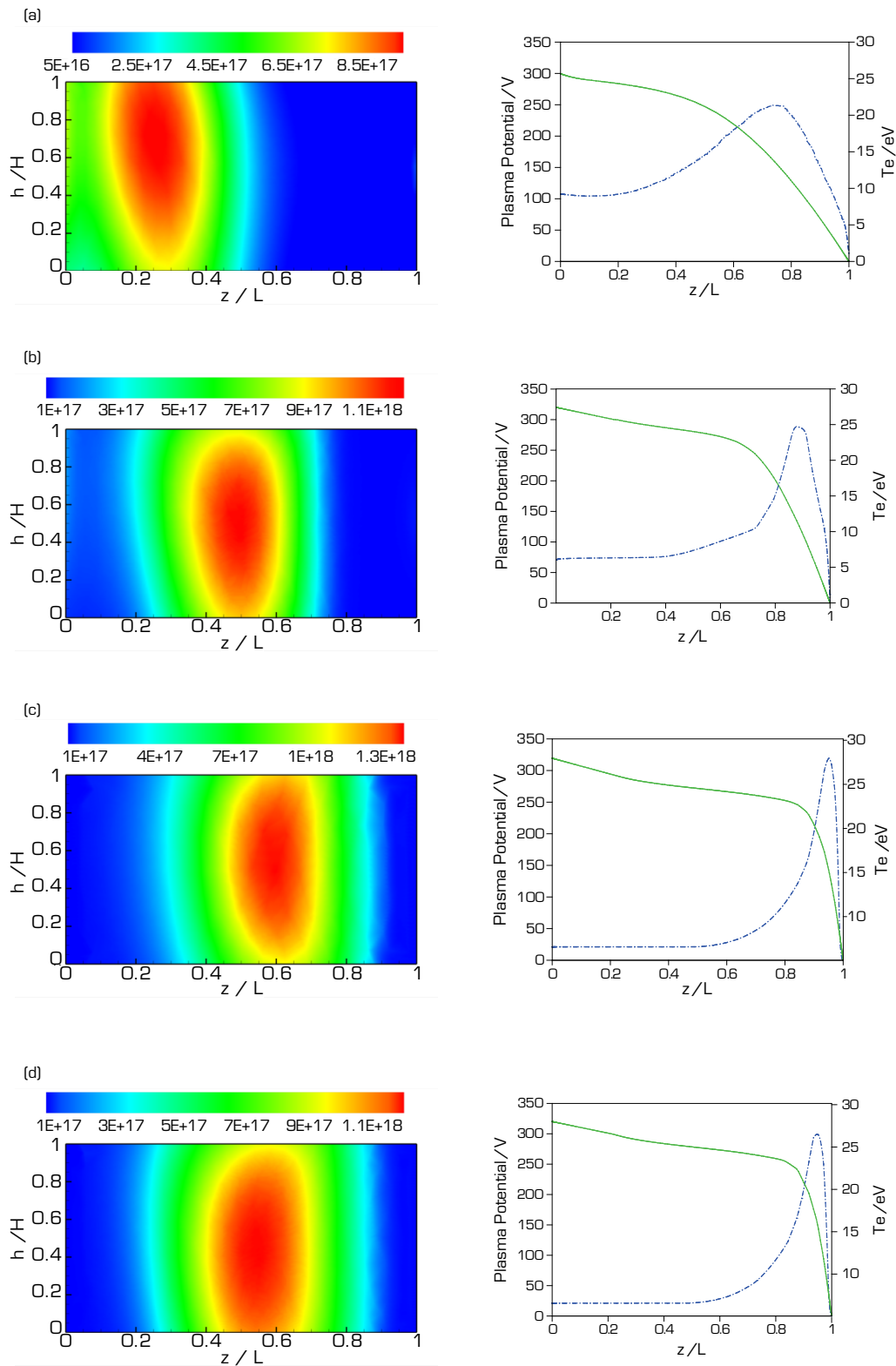
Figure 5 shows the distribution of electron density (left) and plasma potential (right) in different magnetic flux density. When *Br-max* is 110 Gs (shown in Fig. 5a), the peak value of electron temperature is relatively low (shown on the left picture in Fig. 5a), and the area under the high electron temperature curve is larger (shown on the right picture in Fig. 5a). It shows that the magnetic flux density is too weak to restrain the electrons move to the higher potential region, so that the electrons will move towards the anode rapidly and then collide with the neutral atoms. In this case, the ionization reaction mainly occurs near the anode, thus the ionization region is short while the acceleration region is large, and the plasma density will peak close to the anode, which will decrease the efficiency.

In Fig. 5b, the calculation is conducted in the condition of 170 Gs. It can be obviously observed in Fig. 5b (left) that the ionization region moves towards the exit. The peak value of electron temperature is relatively higher than that in Fig. 5a (right), as well as closer to the exit of the channel. Owing to the relatively stronger magnetic flux density near the exit, the electrons residence time becomes longer and the collision frequency with the neutral atoms is increased in turn. So that the ionization efficiency is improved and more atoms and electrons near the exit participate in the ionization reaction in the discharge channel, which results in a longer ionization region and a smaller acceleration region and promotes the utilization of neutral atoms. And then the efficiency of the thruster is also promoted.

Figure 4c shows the results when *Br-max* is 200 Gs. The ionization region locates closer to the exit and acceleration region becomes the smallest in the four conditions.

It can be seen that the ionization region (shown on the left picture in Fig. 5d) moves towards the anode slightly. The peak value of the electron temperature (shown on the right picture in Fig. 5d) is a bit lower than that in Fig. 5c, for that the stronger magnetic flux density costs more electron energy.

The ionization region will be much closer to the exit under proper magnetic flux density, and higher peak value of the electron temperature near the exit will increase the plasma production rate. It can be inferred that the thruster could operate with higher efficiency under the optimized magnetic flux density.

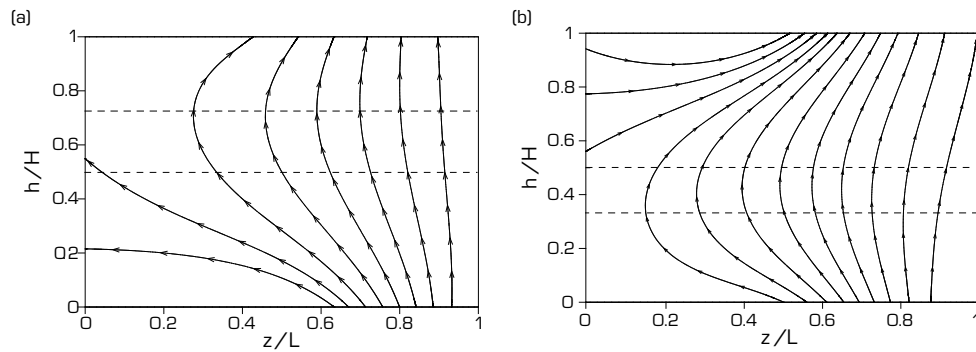


Source: Elaborated by the authors.

Figure 5. Distribution of the electron density in the discharge channel (m^{-3}) and the potential and the electron temperature along the center line of the channel when Br_{-max} is 110 Gs (a), 170 Gs (b), 200 Gs (c), 220 Gs (d).

Effects of the relationship between the magnetic field line and the channel center line

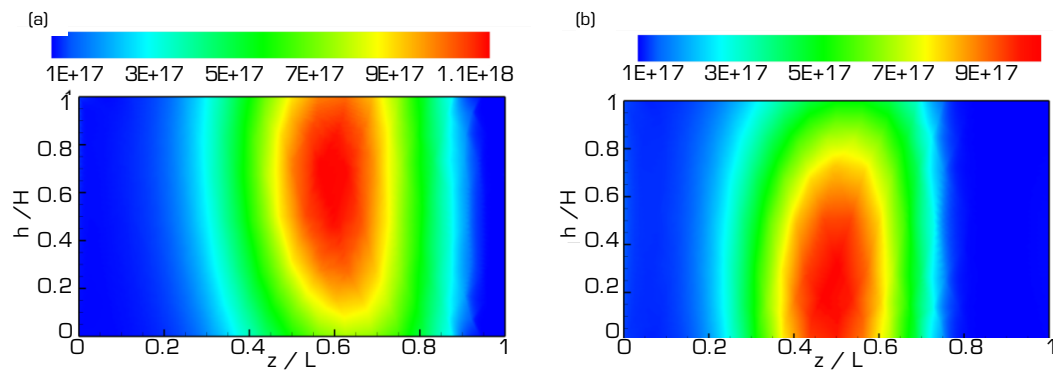
Two kinds of magnetic configuration (B_1 and B_2) have been presented in Fig. 6 to investigate the effects of radial distribution of the magnetic field. Both in Fig. 6a and b, the magnetic field lines are not symmetric about the center line. In Fig. 6a, line of magnetic-curve inflexion is above the center line, videlicet, closer to the outer wall of the channel while it is closer to the inner wall in Fig. 6b.



Source: Elaborated by the authors.

Figure 6. Two kinds of magnetic configurations. (a) B_1 configuration; (b) B_2 configuration.

The corresponding plasma parameters in different magnetic configurations are shown in Fig. 7. The relationship between the magnetic field line and the channel center line influences the discharge characteristic obviously. As shown in Fig. 7a, the maximum electron density locates near the outer wall. The deviation of the plasma distribution will enhance the interaction with the wall, which could increase the energy loss in discharging and decrease the efficiency of the thruster. The strong interaction between the wall and plasma could decrease the efficiency of the discharging (Raitses *et al.* 2005). A similar phenomenon could be observed in B_1 configuration, as shown in Fig. 7b. It can be inferred that the thrust and the efficiency will achieve its peak value when the line of magnetic-curve inflexion coincides with the center line of the channel.



Source: Elaborated by the authors.

Figure 7. Distribution of electron density with different magnetic configurations (m^{-3}). (a) n_e under B_1 configuration; (b) n_e under B_2 configuration.

EXPERIMENTAL RESULTS AND DISCUSSIONS

Experimental apparatus

The experiments were carried out to investigate the influence of the magnetic field on the performance of the low-power hall thruster and confirm the theory of the simulation. All the experiments were conducted in the TS-6A (shown in Fig. 8), which is designed for low-power electric propulsion tests. The thruster was mounted in the main chamber of TS-6A, which has a diameter of 3 m and a length of 5 m. And the vacuum facility could provide an operating pressure of 1×10^{-4} Pa with the hall thruster maximum flow rates. The thrust stand is also used to measure the thrust.



Source: Elaborated by the authors.

Figure 8. The vacuum facility for the experiment.

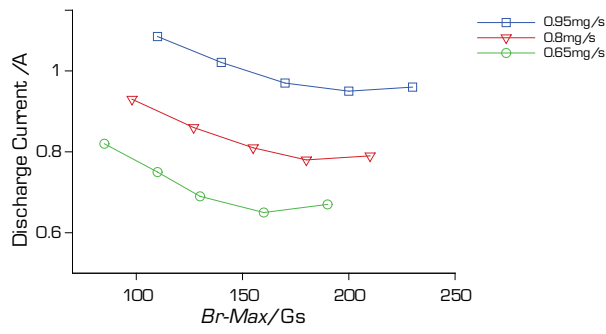
Experimental results

As the magnetic field is produced by a pair of coaxial coils implemented to the thruster, magnetic flux density could be enhanced without changing its configuration by adjusting the exciting current in equal proportion. The operating parameters are listed in Table 2 and the results obtained by experiment are shown in Figs. 9–12. The excitation current chosen for the experiments are obtained by simulation in order to maintain the same magnetic flux density with the simulation conditions.

Table 2. Operating parameters in the experiment.

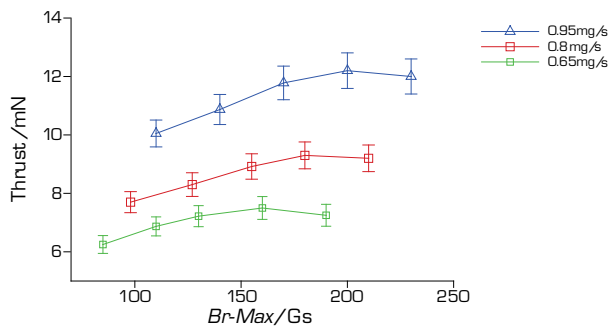
Discharge voltage (V)	Excitation current of inner coil (A)	Excitation current of outer coil (A)
Anode flux rate: $0.95 \text{ mg}\cdot\text{s}^{-1}$		
300	1.56	0.68
300	1.88	0.82
300	2.27	0.98
300	2.70	1.17
300	2.97	1.29
Anode mass flux: $0.8 \text{ mg}\cdot\text{s}^{-1}$		
300	1.39	0.60
300	1.70	0.74
300	2.07	0.89
300	2.43	1.06
300	2.71	1.18
Anode mass flux: $0.65 \text{ mg}\cdot\text{s}^{-1}$		
300	1.21	0.52
300	1.48	0.64
300	1.74	0.75
300	2.16	0.93
300	2.45	1.07

Source: Elaborated by the authors.



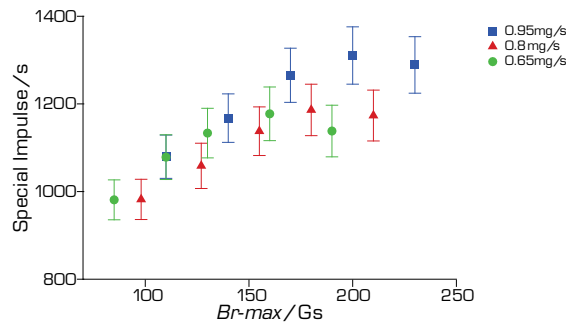
Source: Elaborated by the authors.

Figure 9. The magneto-ampere characteristics.



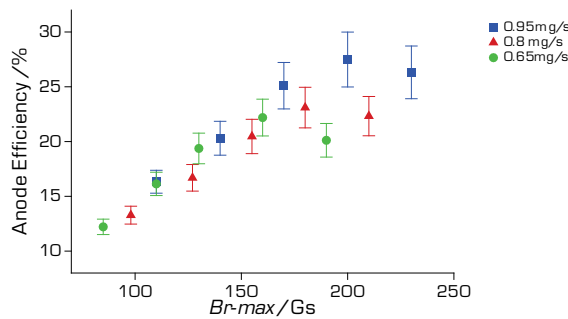
Source: Elaborated by the authors.

Figure 10. The magneto-thrust characteristics.



Source: Elaborated by the authors.

Figure 11. The magneto-special impulse characteristics.



Source: Elaborated by the authors.

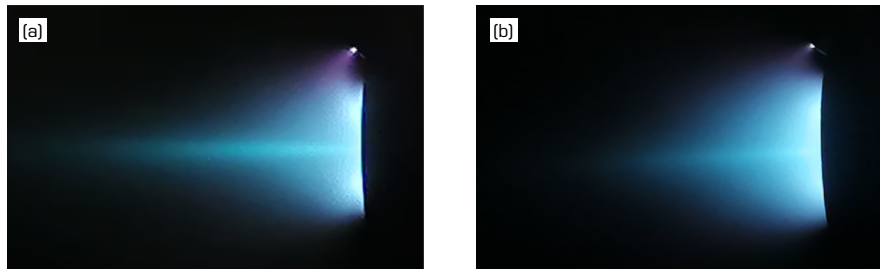
Figure 12. The magneto-efficiency characteristics.

Figure 9 shows the magneto-ampere characteristics. Taking the condition when anode mass flow is $1.7 \text{ mg}\cdot\text{s}^{-1}$ as an example, when the $Br\text{-max}$ is lower than 140 Gs, the discharge current decreased rapidly with the increasing $Br\text{-max}$, while the discharge current almost keep stable when the $Br\text{-max}$ ranging from 170 to 200 Gs. The current rises slowly with the increasing $Br\text{-max}$, when $Br\text{-max} > 200 \text{ Gs}$.

The magneto-thrust characteristic is opposite, shown in Fig. 10. The thrust reaches the extreme value when $Br\text{-max}$ is 200 Gs. As the definition of special impulse, a similar trend is found in Fig. 10. The profile of the magneto-efficiency characteristic in Fig. 12 also presents a similar trend and gets the extreme value when $Br\text{-max}$ is about 200 Gs.

The experiments confirm the speculation of the simulation and indicate that there is an optimal magnetic flux density, where the thruster could operate with the satisfactory efficiency. The LHT-40 obtains the best efficiency 27% when $Br\text{-max}$ is about 200 Gs. The other conditions present a similar tendency. And the optimal magnetic flux density increases with the anode mass flow, which is about 180 Gs for $0.8 \text{ mg}\cdot\text{s}^{-1}$ and 160 Gs for $0.65 \text{ mg}\cdot\text{s}^{-1}$.

The plume shape could also reflect the performance of the thruster to some extent. Figure 13 shows the Hall thruster operating with Xe at 300 V discharge voltage and $0.95 \text{ mg}\cdot\text{s}^{-1}$ anode mass flow under different magnetic flux intensity. It can be found that the low-power hall thruster has a divergent plume, which presents a shape of triangle. The plume in Fig. 13a is longer and narrower than that in Fig. 13b, which indicates that the thruster has a better performance when $Br\text{-max} = 200 \text{ Gs}$. A longer and narrower plume means a smaller divergence-angle, which indicates that more power input to the thruster is converted to generating thrust, which means the efficiency of the thruster is higher (Goebel and Katz 2008). The proper designed magnetic field restrain the plasma away from the wall and concentrated in the center of the discharge channel.



Source: Elaborated by the authors.

Figure 13. The LHT-40 operating under two different kinds of magnetic flux intensity. (a) $Br\text{-max} = 200 \text{ Gs}$; (b) $Br\text{-max} = 110 \text{ Gs}$.

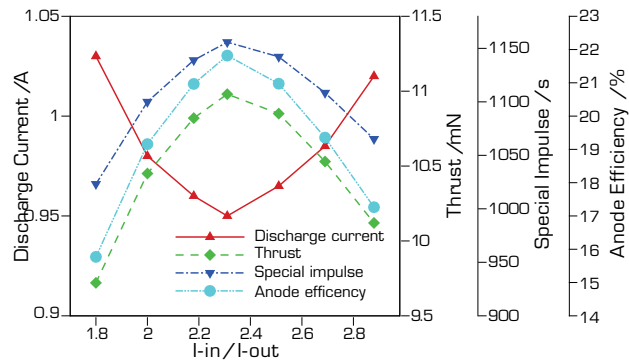
The magnetic configuration is built under the combined action of inner coil and outer coil. So, the exciting current could be adjusted in two coils independently to acquire a series of magnetic configurations. I_{in} and I_{out} are used to represent the excitation current in inner coils and outer coils respectively and the working parameters are listed in Table 3 with $\frac{I_{in}}{I_{out}}$, ranging from 1.8 to 2.9. The discharge voltage is 300 V, and the anode mass flow was set to $1.7 \text{ mg}\cdot\text{s}^{-1}$.

Table 3. Operating parameters in experiment.

I_{in} (A)	I_{out} (A)	I_{in}/I_{out}
2.49	1.38	1.8
2.58	1.29	2.0
2.66	1.22	2.2
2.70	1.17	2.3
2.76	1.10	2.5
2.82	1.05	2.7
2.88	1.00	2.9

Source: Elaborated by the authors.

The experimental results are shown in Fig. 14. It can be inferred that the efficiency reaches the maximum value with the $\frac{I_{in}}{I_{out}}$ at 2.3. The experimental results confirm the theory of the numerical results.



Source: Elaborated by the authors.

Figure 14. Performance of the thruster with different $\frac{I_{in}}{I_{out}}$.

CONCLUSIONS

In order to investigate the influence of the magnetic field on discharge characteristics, numerical method has been adopted as well as experimental method. The effects on the plasma parameters in discharge channel are obtained via established model, such as plasma density, electron temperature and spatial potential. And then experiments were also conducted to investigate the effects on performance.

It can be concluded that, in a proper designed magnetic field, the line of magnetic-curve inflexion in discharge channel should coincide with the center line of the discharge channel to decrease the interaction between the plasma and the wall.

And there is a proper magnetic flux density with which the Hall thruster could achieve its maximum efficiency. The optimal value of the magnetic flux density increases with the increase of anode mass flow. For the LHT-40 hall thruster, the optimal performance was obtained at $0.95 \text{ mg}\cdot\text{s}^{-1}$ anode mass flow, when $Br\text{-max}$ is about 200 Gs, in which the plasma density ranges from 1.0×10^{17} to $1.3 \times 10^{18} \text{ m}^{-3}$ and the thrust is 12.2 mN.

AUTHORS' CONTRIBUTION

Conceptualization: Guo W; **Methodology:** Guo W and Gao J; **Investigation:** Guo W and Gu Z; **Writing – Original Draft:** Guo W; **Writing – Review and Editing:** Gu Z; **Funding Acquisition:** Guo N; **Resources:** Gao J and Guo N; **Supervision:** Gu Z.

DATA AVAILABILITY STATEMENT

The data will be available upon request.

FUNDING

National Natural Science Foundation of China
 [https://doi.org/10.13039/501100001809]
 Grant No. 61901204.

ACKNOWLEDGEMENTS

The authors are thankful to Science and Technology on Vacuum Technology and Physics Laboratory for providing the equipment.

REFERENCES

- Bird RB, Stewart WE, Lightfoot EN (2013) Transport phenomena. 2nd ed. New York: John Wiley & Sons.
- Book DL (1987) NRL plasma formulary. Washington DC: Naval Research Laboratory. <https://doi.org/10.21236/ADA247840>
- Christou AG, Jugroot M (2014) Modeling of an electrical propulsion system: Towards a hybrid system. Paper presented 45th AIAA Plasmadynamics and Lasers Conference. AIAA; Atlanta, Georgia, United States of America. <https://doi.org/10.2514/6.2014-2233>
- Christou AG, Jugroot M (2017) Investigating a two-stage electric space propulsion system: Simulation of plasma dynamics. *Vacuum* 141:22-31. <https://doi.org/10.1016/j.vacuum.2017.03.003>
- Conversano RW, Goebel DM, Mikellides IG, Hofer RR, Matlock TS, Wirz RE (2014) Magnetically shielded miniature hall thruster: Performance assessment and status update. Paper presented 50th AIAA/ASME/SAE/ASEE Joint Propulsion Conference. AIAA; Cleveland, Ohio, United States of America. <https://doi.org/10.2514/6.2014-3896>
- Duan P, Bian X, Cao A, Liu G, Chen L, Yin Y (2016) Effect of segmented electrode length on the performances of an aton-type hall thruster. *Plasma Sci Technol* 18(5):525. <https://doi.org/10.1088/1009-0630/18/5/14>
- Escobar D, Ahedo E (2015) Global stability analysis of azimuthal oscillations in hall thrusters. *IEEE Trans Plasma Sci* 43(1):149-157. <https://doi.org/10.1109/TPS.2014.2367913>
- Gao Y, Liu H, Hu P, Huang H, Yu D (2016) The effect of magnetic field near the anode on cylindrical hall thruster. *Plasma Sources Sci Technol* 25(3):035011. <https://doi.org/10.1088/0963-0252/25/3/035011>
- Garrigues L, Hagelaar GJM, Bareilles J, Boeuf JP (2003) Model study of the influence of the magnetic field configuration on the performance and lifetime of a hall thruster. *Phys Plasmas* 10:4886. <https://doi.org/10.1063/1.1622670>
- Goebel DM, Katz I (2008) Fundamentals of electric propulsion: Ion and hall thrusters. Hoboken: John Wiley & Sons. <https://doi.org/10.1002/9780470436448>
- Grimaud L, Vaudolon J, Mazouffre S, Boniface C (2016) Design and characterization of a 200W hall thruster in “magnetic shielding” configuration. Paper presented 52nd AIAA/ASME/SAE/ASEE Joint Propulsion Conference and Exhibit. AIAA; Salt Lake City, Utah, United States of America. <https://doi.org/10.2514/6.2016-4832>
- Grimaud L, Mazouffre S (2018) Performance comparison between standard and magnetically shielded 200 W Hall thrusters with BN-SiO₂ and graphite channel walls. *Vacuum* 155: 514-523. <https://doi.org/10.1016/j.vacuum.2018.06.056>
- Hofer RR, Gallimore AD (2002) The role of magnetic field topography in improving the performance of high-voltage hall thrusters. Paper presented 38th AIAA/ASME/SAE/ASEE Joint Propulsion Conference and Exhibit. AIAA; Indianapolis, Indiana, United States of America. <https://doi.org/10.2514/6.2002-4111>
- Hofer RR (2004) Development and characterization of high efficiency, high specific impulse xenon hall thrusters (doctoral dissertation). Michigan: University of Michigan. In English.

Katz I, Mikellides IG, Goebel DM (2004) Model of the plasma potential distribution in the plume of a hollow cathode. Paper presented 40th AIAA/ASME/SAE/ASEE Joint Propulsion Conference and Exhibit. AIAA; Fort Lauderdale, Florida, United States of America. <https://doi.org/10.2514/6.2004-4108>

Morozov AI, Esipchuck YV, Kapulkin AM, Nevrovskii VA, Smirnov VA (1972) Effect of the magnetic field on a closed-drift accelerator. *Sov Phys Tech Phys* 17(2):482-487.

Raitses Y, Staack D, Keidar M, Fisch NJ (2005) Electron-wall interaction in hall thrusters. *Phys Plasmas* 12:057104. <http://doi.org/10.1063/1.1891747>

Smirnov A, Raitses Y, Fisch NJ (2002) Parametric investigation of miniaturized cylindrical and annular hall thrusters. *J Appl Phys* 92:5673-5679.

Wang J, Wang Y, Liu Z (2020) [Research on the optimizing effect of the magnetic shield of the hall thruster on the magnetic field]. [*Propulsion Technology*] 41(3):715-720. Chinese. <https://doi.org/10.13675/j.cnki.tjjs.190025>

Yim JT, Keidar M, Boyd ID (2006) An investigation of factors involved in hall thruster wall erosion modeling. Paper presented 42nd AIAA/ASME/SAE/ASEE Joint Propulsion Conference and Exhibit. AIAA; Sacramento, California, United States of America. <https://doi.org/10.2514/6.2006-4657>

Zhang G, Ren J, Jiang Y, Lu C (2018) Design and experiments of a 100 Watt magnetically shielded hall thruster. Paper presented 2018 Joint Propulsion Conference and Exhibit. AIAA; Cincinnati, Ohio, United States of America. <https://doi.org/10.2514/6.2018-4587>